Table 3 Lethal arrhythmias and mortality in an I/R rat model

	Number	VT/VF duration (sec)	Mortality (%)
Saline	7	195±42	71
Empty liposomes	6	162±31	50
Amiodarone (3 mg/kg)	6	167±78	33
Amiodarone (10 mg/kg)	6	36±12*	0#
Liposomal Amiodarone (3 mg/kg)	6	18±9*	0#

*$p<0.05$ versus saline (VT/VF duration). # $p<0.05$ versus saline group (mortality). *VT* ventricular tachycardia, *VF* ventricular fibrillation

Minimal Negative Hemodynamic Effects of Liposomal Amiodarone

Amiodarone causes hypotension and bradycardia in clinical settings [4, 5]. In this study, both free and liposomal amiodarone significantly reduced the HR and systolic BP; however, the time-course changes for both the HR and systolic BP in the liposomal amiodarone group were significantly smaller compared with those following the corresponding dose of free amiodarone. Importantly, the reductions in HR and systolic BP at 1, but not 3, minutes after liposomal amiodarone administration were significantly smaller compared with those following the corresponding dose of amiodarone. These findings suggest that liposomal amiodarone may minimize the negative effects on systemic hemodynamics immediately after the administration of amiodarone. One possible mechanism to explain this finding is that amiodarone on the surface of the liposome membrane is covered with PEG so that amiodarone cannot act directly on cardiovascular cells. Gradual release of amiodarone from liposome may minimize the rapid hemodynamic changes, because systemic hemodynamic effects of liposomal amiodarone were significantly attenuated in liposomal amiodarone group than free amiodarone group.

Augmented Anti-arrhythmic Effects of Liposomal Amiodarone

In this study, liposomal amiodarone (3 mg/kg), but not the corresponding dose of free amiodarone (3 mg/kg), significantly reduced the VT/VF duration and mortality compared with saline in an I/R rat model. Because the acute effects of amiodarone are known to be attributable to blockade of Na^+, Ca^{2+} and dose-dependent K^+ channels [2, 25], increasing the concentration of amiodarone in the I/R myocardium may augment its anti-arrhythmic effects through its tonic effects on cardiomyocytes caused by blocking cardiac ionic currents. Kishida et al. reported that amiodarone enhances nitric oxide production in cultured human endothelial cells [26]. Furthermore, amiodarone protects cardiac myocytes against oxidative injury by scavenging free radicals [27]. These pleiotropic effects of amiodarone are also enhanced by its increased concentration in the I/R myocardium via PEGylated liposomes, which may contribute to the reduction of lethal arrhythmias during reperfusion followed by ischemia. In the present study, since we did not do any procedure such as electrical conversion or cardiac massage for VT/VF, the mortality was higher than in our previous report [16].

Clinical Implications

In clinical settings, higher doses of amiodarone cause hypotension and non-cardiac death or induce worsening heart failure through negative inotropic effects [28]. These effects often diminish the beneficial effects of amiodarone for patients with AMI or heart failure [8, 9]. The present study demonstrated that liposomal amiodarone (3 mg/kg) exerts anti-arrhythmic effects similar to a high dose of free amiodarone (10 mg/kg) while reducing the extent of bradycardia and hypotension, suggesting that encapsulating amiodarone in liposomes augments its anti-arrhythmic effects and reduces its negative effects on hemodynamic parameters with reducing administrative dose. These findings can have a great impact on preventing lethal arrhythmias during reperfusion in AMI patients.

Study Limitations

There are several limitations in this study. We used a brief period of I/R without myocardial infarction in rats. Sakamoto et al. demonstrated that the incidence of VT/VF in a rodent model was 'bell-shaped' with a maximum at 5 min of ischemia and that most lethal arrhythmias occurred within first 20 s after the onset of reperfusion [29]. Consistently, our data showed that the mean time at which the lethal arrhythmia occurred after the onset of reperfusion was 3.3+/−1.6 s. Therefore, we chose the 5 min of ischemia followed by 15 min of reperfusion model. We also chose the timing of drug administration before the onset of ischemia to clarify whether liposomal-amiodarone could prevent the lethal arrhythmia that occurs in the early period of reperfusion. In addition, in clinical practice lethal arrhythmias often occur after a brief period of I/R without any irreversible damage to the heart, indicating that the anti-arrhythmic effects of liposomal amiodarone during a brief period of ischemia model could have clinical relevance [30]. However, careful interpretation is necessary when using liposomal amiodarone in acute myocardial infarction with irreversible damage to confirm the beneficial effects of liposomal amiodarone. Furthermore, because the electrophysiology of rats differs from that of humans and drug administration in our study started before the onset of

ischemia, additional pre-clinical studies including a longer period of I/R model to consider the timing of drug administration are needed using large animal models. We should also take into account that the potential side effects of amiodarone such as bradycardia are minimal in the left coronary artery occlusion model used in the present study.

Conclusion

In conclusion, the targeted delivery of liposomal amiodarone to the I/R myocardium exerted strong anti-arrhythmic effects and reduced the negative impact on systemic hemodynamics. Nano-sized liposomes may be a promising drug delivery system for targeting the I/R myocardium with cardioprotective agents.

Acknowledgments The authors thank Takaki Hayakawa for her technical assistance, Takeshi Aiba for his special advice about data analysis. This research was supported by Grants-in-Aid from the Ministry of Health, Labor, and Welfare of Japan; Grants-in-Aid from the Ministry of Education, Culture, Sports, Science, and Technology of Japan; grants from the Japan Heart Foundation; and grants from the Japan Cardiovascular Research Foundation.

References

1. Di Diego JM, Antzelevitch C. Ischemic ventricular arrhythmias: experimental models and their clinical relevance. Hear Rhythm. 2011;8:1963–8.
2. Kodama I, Kamiya K, Toyama J. Cellular electropharmacology of amiodarone. Cardiovasc Res. 1997;35:13–29.
3. Vassallo P, Trohman RG. Prescribing amiodarone: an evidence-based review of clinical indications. JAMA. 2007;298:1312–22.
4. Scheinman MM, Levine JH, Cannom DS, et al. Dose-ranging study of intravenous amiodarone in patients life-threatening ventricular tachyarrhythmias. The Intravenous Amiodarone Muticenter Investigators Group. Circulation. 1995;92:3264–72.
5. Podrid PJ. Amiodarone; reevaluation of an old drug. Ann Intern Med. 1995;122:689–700.
6. Shiga T, Tanaka T, Irie S, Hagiwara N, Kasanuki H. Pharmacokinetics of intravenous amiodarone and its electrocardiographic effects on healthy Japanese subjects. Hear Vessel. 2011;26:274–81.
7. Wenzel V, Russo SG, Arntz HR, et al. [Comments on the 2010 guidelines on cardiopulmonary resuscitation of the European Resuscitation Council.]. Anaesthesist. 2010.
8. Elizari MV, Martínez JM, Belziti C, et al. Morbidity and mortality following early administration of amiodarone in acute myocardial infarction. GEMICA study investigators, GEMA Group, Buenos Aires, Argentina. Grupo de Estudios Multicentricos en Argentina. Eur Heart J. 2000;21:198–205.
9. Hu K, Gaudron P, Ertl G. Effects of high- and low-dose amiodarone on mortality, left ventricular remodeling, and hemodynamics in rats with experimental myocardial infarction. J Cardiovasc Pharmacol. 2004;44:627–30.
10. Semalty A, Semalty M, Rawat BS, Singh D, Rawat MS. Pharmacosomes: the lipid-based new drug delivery system. Expert Opin Drug Deliv. 2009;6:599–612.
11. Whitehead KA, Langer R, Anderson DG. Knocking down barriers: advances in siRNA delivery. Nat Rev Drug Discov. 2009;8:129–38.
12. Malam Y, Loizidou M, Seifalian AM. Liposomes and nanoparticles: nanosized vehicles for drug delivery in cancer. Trends Pharmacol Sci. 2009;30:592–9.
13. Horwitz LD, Kaufman D, Keller MW, Kong Y. Time course of coronary endothelial healing after injury due to ischemia and reperfusion. Circulation. 1994;90:2439–47.
14. Dauber IM, VanBenthuysen KM, McMurtry IF, et al. Functional coronary microvascular injury evident as increased permeability due to brief ischemia and reperfusion. Circ Res. 1990;66:986–98.
15. Galagudza MM, Korolev DV, Sonin DL, et al. Targeted drug delivery into reversibly injured myocardium with silica nanoparticles: surface functionalization, natural biodistribution, and acute toxicity. Int J Nanomedicine. 2010;5:231–7.
16. Takahama H, Minamino T, Asanuma H, et al. Prolonged targeting of ischemic/reperfused myocardium by liposomal adenosine augments cardioprotection in rats. J Am Coll Cardiol. 2009;53:709–17.
17. Riva E, Hearse DJ. Anti-arrhythmic effects of amiodarone and desethylamiodarone on malignant ventricular arrhythmias arising as a consequence of ischaemia and reperfusion in the anaesthetised rat. Cardiovasc Res. 1989;23:331–9.
18. Canyon SJ, Dobson GP. Protection against ventricular arrhythmias and cardiac death using adenosine and lidocaine during regional ischemia in the in vivo rat. Am J Physiol Heart Circ Physiol. 2004;287:H1286–95.
19. Plomp TA, Wiersinga WM, Maes RA. Tissue distribution of amiodarone and desethylamiodarone in rats after repeated oral administration of various amiodarone dosages. Arzneimittelforschung. 1985;35:1805–10.
20. Feige JN, Sage D, Wahli W, Desvergne B, Gelman L. PixFRET, an ImageJ plug-in for FRET calculation that can accommodate variations in spectral bleed-trhoughs. Microsc Res Tech. 2005;68:51–8.
21. Opitz CF, Mitchell GF, Pfeffer MA, Pfeffer JM. Arrhythmias and death after coronary artery occlusion in the rat. Continuous telemetric ECG monitoring in conscious, untethered rats. Circulation. 1995;92:253–61.
22. Klibanov AL, Maruyama K, Torchilin VP, Huang L. Amphipathic polyethyleneglycols effectively prolong the circulation time of liposomes. FEBS Lett. 1990;268:235–7.
23. Theodossiou TA, Galanou MC, Paleos CM. Novel amiodarone-doxorubicin cocktail liposomes enhance doxorubicin retention and cytotoxicity in DU145 human prostate carcinoma cells. J Med Chem. 2008;51:6067–74.
24. Elhasi S, Astaneh R, Lavasanifar A. Solubilization of an amphiphilic drug by poly(ethylene oxide)-block-poly(ester) micelles. Eur J Pharm Biopharm. 2007;65:406–13.
25. Kamiya K, Nishiyama A, Yasui K, Hojo M, Sanguinetti MC, Kodama I. Short- and long-term effects of amiodarone on the two components of cardiac delayed rectifier K(+) current. Circulation. 2001;9:1317–24.
26. Kishida S, Nakajima T, Ma J, et al. Amiodarone and N-desethylamiodarone enhance endothelial nitric oxide production in human endothelial cells. Int Heart J. 2006;47:85–93.
27. Ide T, Tsutsui H, Kinugawa S, Utsumi H, Takeshita A. Amiodarone protects cardiac myocytes against oxidative injury by its free radical scavenging action. Circulation. 1999;100:690–2.
28. Freedman MD, Somberg JC. Pharmacology and pharmacokinetics of amiodarone. J Clin Pharamacol. 1991;31:1061–9.
29. Sakamoto J, Miura T, Tsuchida A, Fukuma T, Hasegawa T, Shimamoto K. Reperfusion arrhythmias in the murine heart: their characteristics and alteration after ischemic preconditioning. Basic Res Cardiol. 1999;94:489–95.
30. Tzivoni D, Keren A, Granot H, Gottlieb S, Benhorin J, Stern S. Ventricular fibrillation caused by myocardial reperfusion in Prinzmetal's angina. Am Heart J. 1983;105:323–5.

Evaluation of intramitochondrial ATP levels identifies G0/G1 switch gene 2 as a positive regulator of oxidative phosphorylation

Hidetaka Kioka[a,b,1], Hisakazu Kato[a,1], Makoto Fujikawa[c], Osamu Tsukamoto[a], Toshiharu Suzuki[d,e], Hiromi Imamura[f], Atsushi Nakano[a,g], Shuichiro Higo[a,b], Satoru Yamazaki[h], Takashi Matsuzaki[b], Kazuaki Takafuji[i], Hiroshi Asanuma[j], Masanori Asakura[g], Tetsuo Minamino[b], Yasunori Shintani[a], Masasuke Yoshida[e], Hiroyuki Noji[k], Masafumi Kitakaze[g], Issei Komuro[b,l], Yoshihiro Asano[a,b,2], and Seiji Takashima[a,2]

Departments of [a]Medical Biochemistry and [b]Cardiovascular Medicine and [i]Center for Research Education, Osaka University Graduate School of Medicine, Osaka 565-0871, Japan; [c]Department of Biochemistry, Faculty of Pharmaceutical Science, Tokyo University of Science, Chiba 278-8510, Japan; [d]Chemical Resources Laboratory, Tokyo Institute of Technology, Yokohama 226-8503, Japan; [e]Department of Molecular Bioscience, Kyoto Sangyo University, Kyoto 603-8555, Japan; [f]The Hakubi Center for Advanced Research and Graduate School of Biostudies, Kyoto University, Kyoto 606-8501, Japan; Departments of [g]Clinical Research and Development and [h]Cell Biology, National Cerebral and Cardiovascular Center Research Institute, Osaka 565-8565, Japan; [j]Department of Cardiovascular Science and Technology, Kyoto Prefectural University School of Medicine, Kyoto 602-8566, Japan; and [k]Department of Applied Chemistry, School of Engineering and [l]Department of Cardiovascular Medicine, Graduate School of Medicine, University of Tokyo, Tokyo 113-8656, Japan

Edited by Gottfried Schatz, University of Basel, Reinach, Switzerland, and approved November 19, 2013 (received for review October 7, 2013)

The oxidative phosphorylation (OXPHOS) system generates most of the ATP in respiring cells. ATP-depleting conditions, such as hypoxia, trigger responses that promote ATP production. However, how OXPHOS is regulated during hypoxia has yet to be elucidated. In this study, selective measurement of intramitochondrial ATP levels identified the hypoxia-inducible protein G0/G1 switch gene 2 (G0s2) as a positive regulator of OXPHOS. A mitochondria-targeted, FRET-based ATP biosensor enabled us to assess OXPHOS activity in living cells. Mitochondria-targeted, FRET-based ATP biosensor and ATP production assay in a semi-intact cell system revealed that G0s2 increases mitochondrial ATP production. The expression of G0s2 was rapidly and transiently induced by hypoxic stimuli, and G0s2 interacts with OXPHOS complex V (F_oF_1-ATP synthase). Furthermore, physiological enhancement of G0s2 expression prevented cells from ATP depletion and induced a cellular tolerance for hypoxic stress. These results show that G0s2 positively regulates OXPHOS activity by interacting with F_oF_1-ATP synthase, which causes an increase in ATP production in response to hypoxic stress and protects cells from a critical energy crisis. These findings contribute to the understanding of a unique stress response to energy depletion. Additionally, this study shows the importance of assessing intramitochondrial ATP levels to evaluate OXPHOS activity in living cells.

energy metabolism | live-cell imaging

Maintaining cellular homeostasis and activities requires a stable energy supply. Most eukaryotic cells generate ATP as their energy currency mainly through the mitochondrial oxidative phosphorylation (OXPHOS) system. The OXPHOS system consists of five large protein complex units (i.e., complexes I–V), comprising more than 100 proteins. In this system, oxygen (O_2) is essential as the terminal electron acceptor for complex IV to finally produce the proton-motive force that drives the ATP-generating molecular motor complex V (F_oF_1-ATP synthase).

Hypoxia causes the depletion of intracellular ATP and triggers adaptive cellular responses to help maintain intracellular ATP levels and minimize any deleterious effects of energy depletion. Although the metabolic switch from mitochondrial respiration to anaerobic glycolysis is widely recognized (1–4), several recent reports have shown that hypoxic stimuli unexpectedly increase OXPHOS efficiency as well (5–7). In other words, cells have adaptive mechanisms to maintain intracellular ATP levels by enhancing OXPHOS, particularly in the early phase of hypoxia, in which the O_2 supply is limited but still remains. However, the mechanism by which OXPHOS is regulated during this early hypoxic phase is still not fully understood.

Revealing the mechanism of this fine-tuned regulation of OXPHOS requires accurate and noninvasive measurements of OXPHOS activity. Although researchers have established methods to measure OXPHOS activity, precise measurement, especially in living cells, is still difficult. Measuring the intracellular ATP concentration is one of the most commonly used methods for evaluating OXPHOS activity. However, there are two major problems with this method. First, the intracellular ATP concentration does not always accurately reflect OXPHOS activity, because it can also be affected by glycolytic ATP production, cytosolic ATPases, and ATP buffering enzymes, such as creatine kinase and adenylate kinase (8). Second, because measurements of the ATP concentration by chromatography (9), MS (10), NMR (11), or luciferase assays (12) are based on cell extract analysis, these methods cannot be used to measure the serial ATP concentration changes in living cells in real time.

In this study, we overcame these problems by the selective measurement of the intramitochondrial matrix ATP concentration ($[ATP]_{mito}$) in living cells. In the final step of OXPHOS, ATP is produced not in the cytosol but in the mitochondrial matrix. Therefore, we hypothesized that a selectively measuring $[ATP]_{mito}$ is suitable for the highly sensitive evaluation of cellular ATP production by OXPHOS. In fact, real-time evaluation of both $[ATP]_{mito}$ and the cytosolic ATP concentration ($[ATP]_{cyto}$) in living cells revealed that $[ATP]_{mito}$ reflected OXPHOS activity with far more sensitivity than $[ATP]_{cyto}$. Using this fine method, we found that G0/G1 switch gene 2 (G0s2), a hypoxia-induced

Significance

We developed a sensitive method to assess the activity of oxidative phosphorylation in living cells using a FRET-based ATP biosensor. We then revealed that G0/G1 switch gene 2, a protein rapidly induced by hypoxia, increases mitochondrial ATP production by interacting with F_oF_1-ATP synthase and protects cells from a critical energy crisis.

Author contributions: Y.A. and S.T. designed research; H. Kioka, H. Kato, O.T., and A.N. performed research; M.F., T.S., H.I., S.H., S.Y., T. Matsuzaki, K.T., H.A., M.A., T. Minamino, Y.S., M.Y., H.N., M.K., and I.K. contributed new reagents/analytic tools; H. Kioka and H. Kato analyzed data; and Y.A. and S.T. wrote the paper.

The authors declare no conflict of interest.

This article is a PNAS Direct Submission.

[1]H. Kioka and H. Kato contributed equally to this work.

[2]To whom correspondence may be addressed. E-mail: asano@cardiology.med.osaka-u.ac.jp or takasima@cardiology.med.osaka-u.ac.jp.

This article contains supporting information online at www.pnas.org/lookup/suppl/doi:10.1073/pnas.1318547111/-/DCSupplemental.

protein in cardiomyocytes, increases OXPHOS activity. G0s2 interacted with F_oF_1-ATP synthase and increased the ATP production rate. Our results suggest that hypoxia-induced protein G0s2 is a positive regulator of OXPHOS and protects cells by preserving ATP production, even under hypoxic conditions.

Results

Establishment of a Sensitive Method to Assess OXPHOS Activity in Living Cells. To elucidate the mechanism by which OXPHOS is regulated under hypoxia, it is essential to establish a sensitive method for assessing OXPHOS activity in living cells. For this purpose, we used an ATP indicator based on ε-subunit for analytical measurements (ATeam), which is an ATP-sensing FRET-based indicator (13). We introduced this ATP biosensor into cardiomyocytes that possess an abundance of mitochondria and produce the highest levels of ATP among all primary cells (14, 15). The ATeam assay can measure both $[ATP]_{cyto}$ (i.e., the Cyto-ATeam assay) and $[ATP]_{mito}$ when a duplex of the mitochondrial targeting signal of cytochrome *c* oxidase subunit VIII is attached to the indicator (i.e., the Mit-ATeam assay). In this case, the YFP/CFP emission ratio of the ATeam fluorescence represents the ATP concentration in each compartment. Interestingly, the Mit-ATeam assay was a far more sensitive method than the Cyto-ATeam assay in determining OXPHOS activity in living cells. For example, a very low dose of oligomycin A (0.01 μg/mL), a specific OXPHOS complex V (F_oF_1-ATP synthase) inhibitor, greatly reduced the YFP/CFP emission ratio of the Mit-ATeam fluorescence that represents $[ATP]_{mito}$ within 10 min (Fig. 1 *A*, *Upper* and *B* and Movie S1). In contrast, the same dose of oligomycin A resulted in a slight and slow decline of the YFP/CFP emission ratio of Cyto-ATeam fluorescence (Fig. 1 *A*, *Lower* and *B* and Movie S1). The same phenomenon was observed when the cells were exposed to hypoxia, which suppresses the activity of OXPHOS complex IV (cytochrome *c* oxidase). Again, $[ATP]_{mito}$ decreased more markedly than $[ATP]_{cyto}$ during 2.5 h of hypoxia (Fig. 1 *C* and *D* and Movie S2). These results indicate that the Mit-ATeam assay is far more sensitive for measuring the activity of OXPHOS than the Cyto-ATeam assay. In addition, OXPHOS inhibition decreased the YFP/CFP emission ratio of the Mit-ATeam fluorescence of HeLa cells as well as cardiomyocytes (Fig. S1), suggesting the broad applicability of this assay. Therefore, we used Mit-ATeam for the assessment of the OXPHOS activity in living cells.

Hypoxia-Induced Gene G0s2 Affects the Intramitochondrial ATP Concentration. The expression of genes involved in OXPHOS regulation is considered to be up-regulated in the early phase of hypoxia. Thus, to find unique OXPHOS regulators, we focused on the rapidly induced genes in response to hypoxic stimulation. We compared the gene expression profiles of cultured rat cardiomyocytes at three different time points during hypoxic conditions (0, 2, and 12 h) (Fig. S2*A*). The expression of well-known hypoxia-induced genes, such as VEGF-α and hexokinase 2 mRNA (16, 17), was slightly up-regulated at 2 h and further enhanced at 12 h of hypoxia. In contrast, three other genes (*Adamts1*, *Cdkn3*, and *G0s2*) underwent rapid increases in expression at 2 h but declined at 12 h of sustained hypoxia (Fig. S2 *B* and *C*). This rapid and transient time course of expression implies that these three genes may play distinct regulatory roles, especially in the early hypoxic phase, in which oxygen is limited but still available. To examine whether these genes are involved in the regulation of OXPHOS activity, we knocked down these genes by shRNA (see Fig. S7*A*) and examined $[ATP]_{mito}$ using the Mit-ATeam assay. In this experiment, $[ATP]_{mito}$ in cardiomyocytes treated with shRNA for G0s2 clearly declined within 24 h compared with the control cardiomyocytes (Fig. 2*A* and Movie S3). In addition, the time course of ATP decline was in agreement with the time course of G0s2 depletion (Fig. 2*A* and Fig. S3*A*). Importantly, the overexpression of G0s2 restored normal ATP levels (Fig. 2 *B* and *C*), and again, the Cyto-ATeam assay could not detect a significant effect of G0s2 knockdown within this time frame (Fig. S3*B* and Movie S4). These findings imply that mitochondrial ATP production through OXPHOS was inhibited by G0s2 ablation. We confirmed that the mRNA and protein levels of G0s2 both increased after 2–6 h of hypoxia and then declined after 12 h of hypoxia (Fig. 2 *D* and *E*). G0s2 was first reported as a gene with

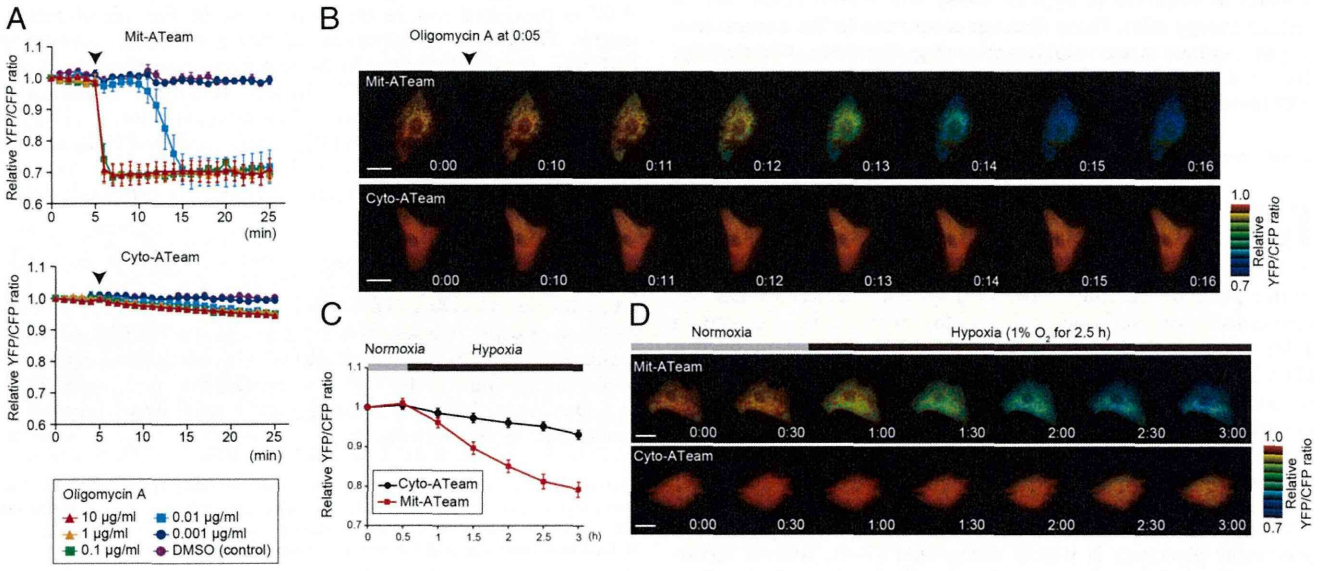

Fig. 1. Establishment of a sensitive method to assess OXPHOS activity in living cells. (*A*) YFP/CFP emission ratio plots of (*Upper*) Mit-ATeam and (*Lower*) Cyto-ATeam fluorescence in cardiomyocytes. Various concentrations (0.001, 0.01, 0.1, 1, and 10 μg/mL) of oligomycin A or DMSO (control) were added at 5 min (arrowhead; $n = 3$). (*B*) Representative sequential YFP/CFP ratiometric pseudocolored images of (*Upper*) Mit-ATeam and (*Lower*) Cyto-ATeam in cardiomyocytes. Oligomycin A (0.01 μg/mL) was added at 5 min. (Scale bars: 20 μm.) (*C*) YFP/CFP emission ratio plots of Mit-ATeam and Cyto-ATeam fluorescence in cardiomyocytes ($n = 10$). (*D*) Representative sequential YFP/CFP ratiometric pseudocolored images of (*Upper*) Mit-ATeam and (*Lower*) Cyto-ATeam in cardiomyocytes. Cells were exposed to 1% hypoxia from the time point 30 min. All of the measurements were normalized to the YFP/CFP emission ratio at 0 min. Data are represented as the means ± SEMs. (Scale bars: 20 μm.)

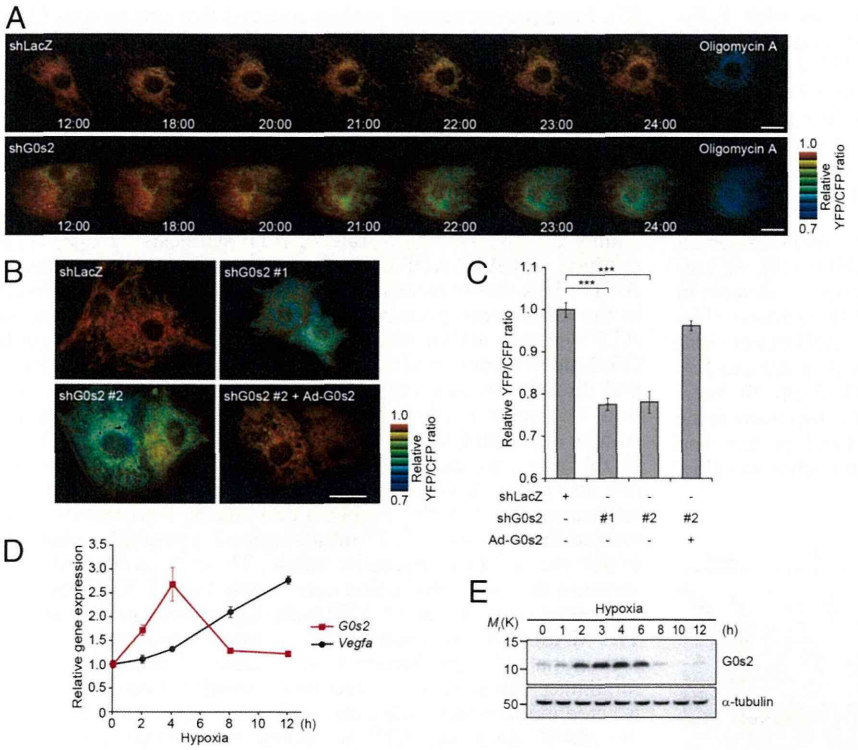

Fig. 2. G0s2, a hypoxia-inducible protein, affects intramitochondrial ATP concentration in cardiomyocytes. (*A*) Sequential YFP/CFP ratiometric pseudocolored images of Mit-ATeam fluorescence in cardiomyocytes expressing (*Upper*) shRNAs for LacZ (shLacZ) or (*Lower*) G0s2 (shG0s2). Oligomycin A (1 μg/mL) was added at the end of the time-lapse imaging to completely inhibit ATP synthesis. The indicated time represents the period after adenovirus infection. (*B*) Representative YFP/CFP ratiometric pseudocolored images of Mit-ATeam fluorescence in cardiomyocytes expressing the indicated adenovirus for 24 h. (Scale bar: *A* and *B*, 20 μm.) (*C*) The bar graph shows the mean YFP/CFP emission ratio of Mit-ATeam fluorescence in cardiomyocytes expressing shLacZ (n = 30), shG0s2 #1 (n = 30), shG0s2 #2 (n = 29), and shG0s2 #2 + G0s2 WT (n = 32) for 24 h. All of the measurements were normalized to the average of the control cells (shLacZ). ***$P < 0.001$. (*D*) Gene expression value plots of *G0s2* (red line) and *VEGF-α* (*Vegfa*; black line) levels in cardiomyocytes under hypoxic conditions (1% O_2). Each value was compared with the level of *Actb* expression (n = 3). Values represent the means ± SEMs. (*E*) Immunoblotting of the G0s2 expression in cardiomyocytes under hypoxic conditions (1% O_2).

expression that was induced during the cell cycle switch from G0 to G1 phase (18). G0s2 is expressed in many tissues and especially abundant in heart, skeletal muscle, liver, kidney, brain, and adipose tissue (19). Although G0s2 may play a role in cell cycle progression (20), the function of G0s2 in the hypoxic response remains unknown.

G0s2 Rescues the Decline of ATP Production During Hypoxia. We next tested whether the overexpression of the G0s2 before hypoxic stress could prevent hypoxia-induced ATP depletion. We prepared cardiomyocytes overexpressing G0s2 and control cardiomyocytes. During sustained hypoxia, $[ATP]_{mito}$ gradually declined in control cardiomyocytes as measured by the Mit-ATeam assay. Notably, the overexpression of G0s2 before the onset of hypoxia reduced this decline in $[ATP]_{mito}$, which allowed the cardiomyocytes to promptly recover to baseline levels of $[ATP]_{mito}$ after reoxygenation (Fig. 3 *A* and *B* and Movie S5). In addition, the prehypoxia overexpression of G0s2 preserved cell viability during sustained hypoxia (Fig. 3*C*). These results suggest that G0s2 can preserve mitochondrial ATP production even under hypoxia and protect cells from the energy crisis under hypoxia.

G0s2 Binds to F_oF_1-ATP Synthase but Not Other OXPHOS Protein Complexes. To reveal the mechanism by which G0s2 affects $[ATP]_{mito}$, we sought to identify the biochemical targets of G0s2. We screened for G0s2 binding proteins by immunoaffinity purification of cell lysates from cardiomyocytes expressing C-terminally Flag-tagged G0s2 (G0s2-Flag). G0s2-Flag is expressed in cardiomyocytes localized to the mitochondria (Fig. S4*A*). MS analysis revealed that multiple F_oF_1-ATP synthase subunits, but no other mitochondrial respiratory chain complex subunits, were coimmunoprecipitated with G0s2-Flag (Fig. S4*B* and Table S1). F_oF_1-ATP synthase is a well-known ATP-producing enzyme composed of a protein complex that contains an extramembranous F_1 and an intramembranous F_o domain linked by a peripheral and a central stalk (21–24). The binding of F_oF_1-ATP synthase to G0s2-Flag was confirmed by immunoblotting with antibodies against several subunits of F_oF_1-ATP synthase (Fig. 4*A*).

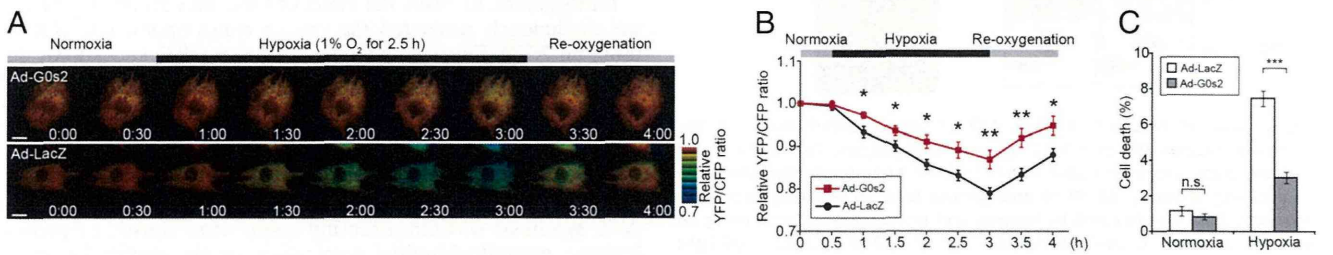

Fig. 3. Overexpression of G0s2 before hypoxia rescues the decline of mitochondrial ATP production during hypoxia. (*A*) Sequential YFP/CFP ratiometric pseudocolored images of Mit-ATeam fluorescence in cardiomyocytes expressing (*Upper*) G0s2 WT or (*Lower*) LacZ during hypoxia and reoxygenation. (Scale bar: 20 μm.) (*B*) YFP/CFP emission ratio plots of Mit-ATeam fluorescence in cardiomyocytes expressing G0s2 WT (n = 20) or LacZ (n = 19) during hypoxia and reoxygenation. All of the measurements were normalized to the ratio at time 0 and compared between cardiomyocytes with G0s2 WT and LacZ at each time point. (*C*) The bar graph shows the cell viability of cardiomyocytes overexpressing G0s2 under hypoxic conditions. Cardiomyocytes expressing either LacZ or G0s2 WT were cultured under normoxic or hypoxic conditions for 18 h (n = 8). The asterisks denote statistical significance comparing G0s2 with LacZ. Data are represented as the means ± SEMs. n.s., not significant. *$P < 0.05$; **$P < 0.01$; ***$P < 0.001$.

Conversely, G0s2-Flag was coimmunoprecipitated with F_oF_1-ATP synthase (Fig. S4*C*). G0s2-Flag was also found to be associated with the F_oF_1-ATP synthase in 293T and HeLa cells (Fig. S4*C*). Both coimmunoprecipitation using an anti-G0s2 antibody and a reciprocal immunoprecipitation revealed that endogenous G0s2 interacts with F_oF_1-ATP synthase, whereas none of the proteins in complexes I–IV or adenine nucleotide translocase 1 (ANT1; also referred to as ADP/ATP carrier) were coimmunoprecipitated with G0s2 (Fig. 4 *B* and *C*).

Given that the G0s2 protein contains an evolutionarily conserved amino terminus and one hydrophobic domain (HD) (19), we created three G0s2 partial deletion mutants to identify the domain in G0s2 that is important for binding to F_oF_1-ATP synthase (Fig. S4*D*). Among these mutants, G0s2 ΔC and G0s2 ΔN but not G0s2 ΔHD bound to the F_oF_1-ATP synthase complex (Fig. 4*D* and Fig. S4 *E* and *F*). Furthermore, we confirmed that G0s2 directly interacts with F_oF_1-ATP synthase in an in vitro pull-down assay using a recombinant maltose-binding protein–fused G0s2 protein and purified F_oF_1-ATP synthase from bovine heart mitochondria (Fig. S5). Immunocytochemical analysis revealed that endogenous G0s2 colocalized with the β-subunit of F_oF_1-ATP synthase (Fig. 4*E*). The knockdown of G0s2 expression by shRNA abolished G0s2 staining (Figs. S6 and S7*A*), indicating that both antibodies used for immunostaining specifically recognize G0s2. These data suggest that G0s2 interacts with the F_oF_1-ATP synthase complex through its HD in mitochondria and regulates OXPHOS activity.

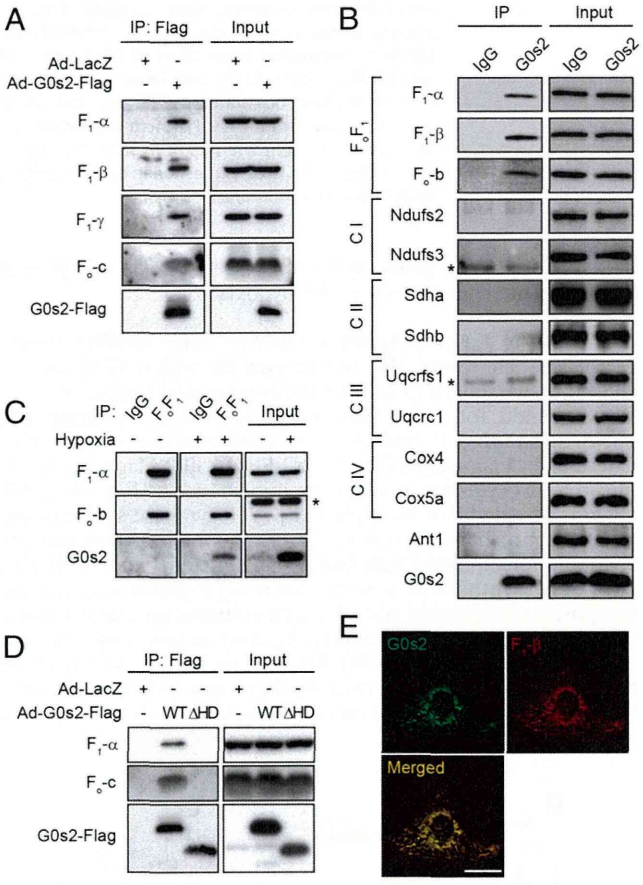

Fig. 4. G0s2 interacts with the F_oF_1-ATP synthase in mitochondria. (*A*) Immunoprecipitation (IP) of G0s2-Flag in cardiomyocytes. Cell lysates from cardiomyocytes expressing G0s2-Flag or LacZ were immunoprecipitated with an anti-Flag antibody. (*B*) IP of endogenous G0s2 in cardiomyocytes. Endogenous G0s2 was induced by hypoxia and immunoprecipitated using an anti-G0s2 antibody. C, OXPHOS complex; F_oF_1, F_oF_1-ATP synthase. *IgG light chain. (*C*) IP of F_oF_1-ATP synthase in cardiomyocytes under normoxic or hypoxic conditions. Cell lysates from cardiomyocytes cultured under normoxia or hypoxia for 4 h were immunoprecipitated with an antibody against the whole F_oF_1-ATP synthase complex or a control IgG. *Nonspecific band. (*D*) IP of G0s2 mutants expressed in cardiomyocytes. Cell lysates were immunoprecipitated with an anti-Flag antibody. (*E*) Immunostained images of hypoxia-stimulated (4 h) cardiomyocytes with anti-G0s2 (green) and anti–F_oF_1-ATP synthase β-subunit (red) antibodies. (Scale bars: 20 μm.)

G0s2 Increases Mitochondrial ATP Production Rate. $[ATP]_{mito}$ is mainly determined by the rate of ATP synthesis by F_oF_1-ATP synthase and ATP/ADP exchange by the ATP/ADP translocase ANT1. This theory means that the increased $[ATP]_{mito}$ observed in the G0s2-overexpressing cells may result from the increased ATP synthesis and/or decreased ATP/ADP exchange, although G0s2 did not interact with ANT1 (Fig. 4*B*). To resolve this issue and directly measure the rate of ATP production in mitochondria, we used a semiintact cell system called the mitochondrial activity of streptolysin O permeabilized cells (MASC) assay (25). In this assay, we permeabilized the plasma membrane to wash out any cytosolic components, such as creatine and glycolytic substrates, but left the mitochondria intact. Furthermore, we treated the cells with P^1, P^5-di(adenosine-5′) pentaphosphate to inhibit the activity of adenylate kinase. These steps allowed us to measure the ATP production rate mostly from OXPHOS, with a minimal contribution of ATP buffering systems in the cytosol. The MASC assay was suitable for accurate measurement of mitochondrial ATP production rate, because mitochondria in this semiintact cell system suffered much smaller damage than the isolated mitochondria in the conventional method. Surprisingly, in the MASC assay, the ATP production rate markedly increased when G0s2 was expressed in HeLa cells that lacked endogenous G0s2 (Fig. 5*A*). In cardiomyocytes, shRNA-mediated G0s2 knockdown decreased the ATP production rate in mitochondria, and the expression of G0s2 WT but not G0s2 ΔHD could restore the ATP production rate (Fig. 5*B* and Fig. S7*A*). In both cells, complete inhibition of ATP production by oligomycin A indicated that the observed ATP synthesis was catalyzed by OXPHOS but not other metabolism (Fig. 5 *A* and *B*).

Next, to evaluate the physiological role of G0s2, we examined whether endogenous G0s2 induced by hypoxia could enhance the ATP production rate. Cardiomyocytes were pretreated with hypoxia for 4 h, during which G0s2 expression was largely induced. We then evaluated the ATP production rate of both hypoxia-pretreated and nontreated cardiomyocytes under room air conditions. Even under these equivalent normoxic conditions, hypoxia-pretreated cardiomyocytes produced ATP faster than nontreated control cardiomyocytes (Fig. 5*C* and Fig. S7*B*). G0s2 knockdown attenuated this increase in the rate of ATP production, indicating that the enhanced ATP production rate resulting from hypoxia pretreatment primarily depends on endogenous G0s2 induction. This increased G0s2 expression was essential for cell survival, because G0s2-depleted cells died earlier than control cells under conditions of hypoxic stress (Fig. 5*D*)

Furthermore, to assess the effect of G0s2 on cellular respiration, we continuously measured the oxygen consumption rate (OCR) using an XF96 Extracellular Flux Analyzer. G0s2 knockdown decreased the basal OCR of cardiomyocytes, most likely because of the decreased activity of ATP synthesis (Fig. 5 *E* and *F*). In contrast, the proton leakage of the mitochondrial inner membrane and the maximum respiratory capacity of OXPHOS complexes I–IV were unaffected by G0s2 ablation (Fig. 5 *E* and *F*). These data show that G0s2 knockdown reduced respiration caused by ATP synthesis without affecting respiration caused by proton leakage, nonmitochondrial respiration, or the maximal respiration capacity.

All these findings indicate that G0s2 enhances the mitochondrial ATP production rate by increasing the activity of F_oF_1-ATP synthase.

Discussion

In this study, we showed that G0s2 kinetically increased OXPHOS activity through direct binding to F_oF_1-ATP synthase. Our previous

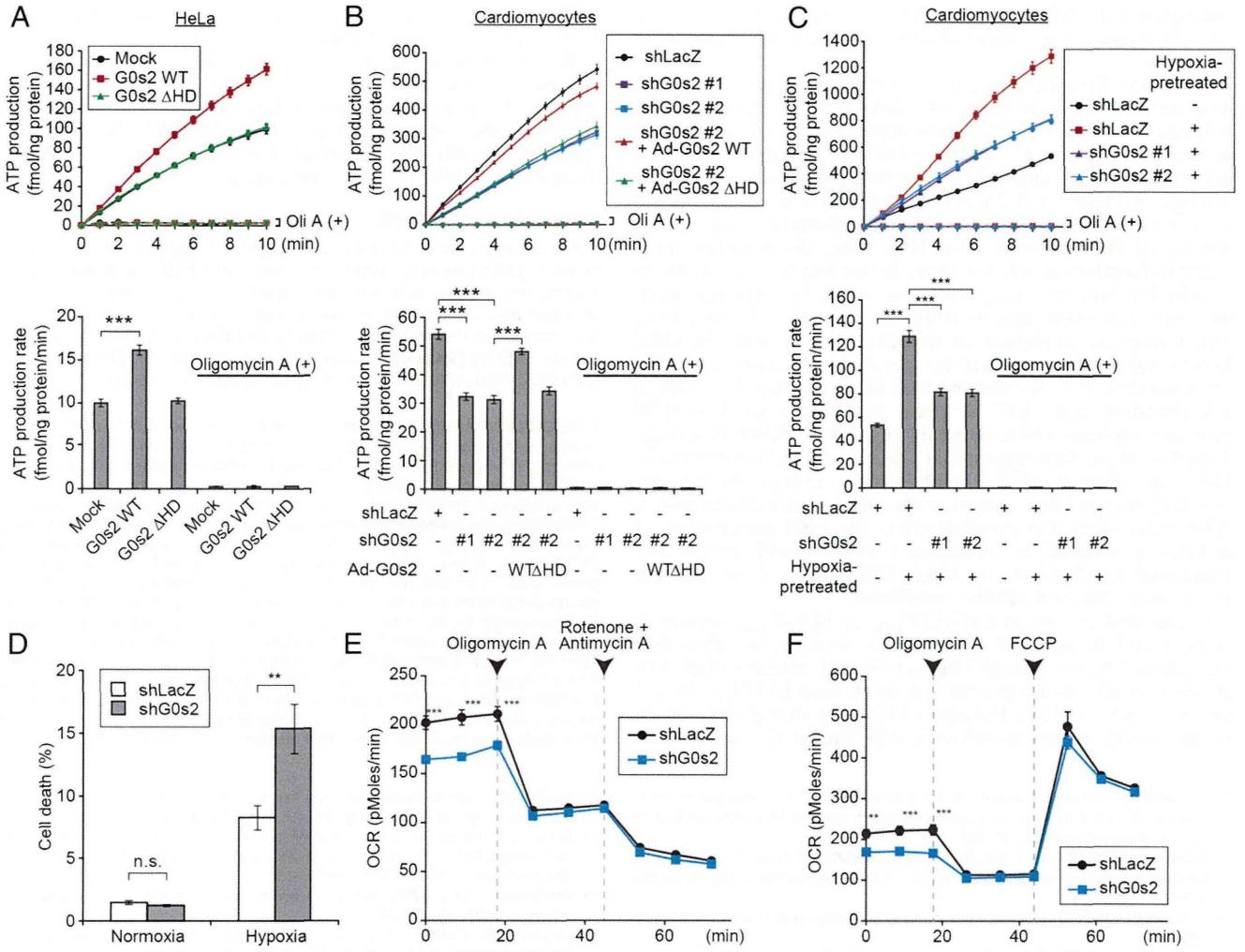

Fig. 5. G0s2 enhances the mitochondrial ATP production rate. (*A* and *B*) MASC assay of (*A*) permeabilized HeLa cells expressing the indicated plasmids or (*B*) cardiomyocytes expressing the indicated adenovirus in the presence (dotted lines) or absence (solid lines) of 1 μg/mL oligomycin A (Oli A). *Upper* shows the ATP production plots, and *Lower* shows the mean ATP production rates between 0 and 10 min. (*A*) $n = 12$. (*B*) Solid lines, $n = 12$; dotted lines, $n = 8$. (*C*) MASC assay of permeabilized cardiomyocytes pretreated with hypoxia. Cells expressing the indicated adenovirus were pretreated with or without hypoxia for 4 h. After the pretreatment, the cells were permeabilized under room air conditions followed by MASC assay in the presence (dotted lines; $n = 8$) or absence (solid lines; $n = 12$) of 1 μg/mL Oli A. *Upper* shows the ATP production plot, and *Lower* shows the mean ATP production rate between 0 and 10 min. (*D*) The bar graph represents the cell viability of G0s2-depleted cardiomyocytes under hypoxic conditions. Cardiomyocytes expressing shLacZ or shG0s2 (#2) were cultured under normoxic or hypoxic conditions for 18 h. (*E* and *F*) The OCR in cardiomyocytes expressing shLacZ and shG0s2 (#2) under basal conditions and in response to the indicated mitochondrial inhibitors ($n = 8$). FCCP, carbonyl cyanide-4-(trifluoromethoxy)-phenylhydrazone. Data are represented as the means ± SEMs. n.s., not significant. $^{**}P < 0.01$; $^{***}P < 0.001$.

studies of F_oF_1-ATP synthase have revealed that this enzyme has a specific structure that connects two molecular nanomotors that synchronize with each other to produce ATP (26–30). These physically distinct structures suggest that a specific activating factor for F_oF_1-ATP synthase must exist. Combined with the findings from this study, we hypothesize that G0s2 may lower the activation barrier of the F_oF_1-ATP synthase nanomotor and enhance the ATP production rate with the equivalent proton motive driving force (PMF; i.e., the sum of the membrane potential and the pH gradient). Activation barriers might be generated by various factors, such as friction between the stator and rotor of F_oF_1-ATP synthase, physical and electrical resistance to proton transport through the channel, and the existence of rotary blockers such as the bacterial ε-subunit and cyclophilin D (31). The increased ATP production rate caused by G0s2 overexpression observed in the MASC assay supports this hypothesis, because the PMF in the initial phase of this assay should be the same. If this hypothesis is true, even with reduced PMF, cells that express G0s2 should produce ATP faster than cells that express little or no G0s2. In fact, G0s2 overexpression attenuated the decline of $[ATP]_{mito}$ under hypoxic conditions that reduced the PMF. Precise real-time measurement of the PMF is currently difficult, but these hypotheses might be proven in future studies. Kinetically faster ATP production should accompany greater consumption of both O_2 and PMF; however, our results suggest that preserving ATP production is more beneficial than preserving PMF for cell viability, particularly when the O_2 supply is restricted but still exists. The transience of endogenous G0s2 expression induced by hypoxia might serve to protect tissues in the early phase of energy crisis. There may be specific mechanisms to decrease G0s2 expression under prolonged ischemia that have yet to be identified. Another possible mechanism by which G0s2 could increase the ATP production rate is that G0s2 increases the F_o-F_1 coupling efficiency of F_oF_1-ATP synthase. However, this hypothesis is less likely, because G0s2 altered the oxygen consumption rate to increase the ATP production rate. Although this uncoupling phenomenon has rarely been reported for mammalian mitochondrial F_oF_1-ATP synthase, we cannot completely eliminate the possibility that intrinsically

uncoupled F_oF_1-ATP synthase exists, because we could not accurately measure the amount of uncoupled F_oF_1-ATP synthase in intact cells.

G0s2 was first identified in cultured monocytes during the drug-induced cell cycle transition from G0 to G1 phase (18, 32). A limited number of studies have implied that G0s2 is involved in cell proliferation (33), differentiation (19), apoptosis (34), inflammation (35), and lipid metabolism (36) in various cellular settings. Moreover, G0s2 was reported to localize to the cytosol (33), endoplasmic reticulum (19), mitochondria (34), or the surface of lipid droplets (36). How G0s2 distinguishes these multiple functions is still not clear. In our hands, G0s2 is always localized to mitochondria, which was shown by immunostaining with two antibodies against different epitopes of G0s2 (Fig. S6). Complete depletion of mitochondrial staining by G0s2 knockdown strongly suggests the specific localization of G0s2 to mitochondria. We also showed that G0s2 specifically bound to mitochondrial F_oF_1-ATP synthase but not other OXPHOS protein complexes and functionally regulated OXPHOS activity. Together, these data suggest that G0s2 acts in the mitochondria. However, different cellular conditions may change the localization and role of G0s2. Additionally, G0s2-mediated changes in ATP metabolism may possibly affect the lipid metabolism or cellular proliferation. Additional studies will reveal the functional mechanisms by which G0s2 exerts these multiple functions in different cellular conditions.

In this study, we evaluated $[ATP]_{mito}$ and $[ATP]_{cyto}$ separately using FRET-based ATP biosensors in living cells. This dual evaluation revealed that $[ATP]_{mito}$ reflected mitochondrial ATP production with much greater sensitivity than $[ATP]_{cyto}$ (Fig. 1 and Movies S1 and S2). Because $[ATP]_{cyto}$ is strongly influenced by the activity of various cytosolic ATP hydrolytic enzymes and ATP buffering enzymes, $[ATP]_{cyto}$ does not always reflect the ATP availability that determines cellular function.

Taken together, our results indicate that G0s2 is a positive regulator of OXPHOS that works to increase the mitochondrial ATP production rate even under hypoxic conditions. Therefore, enhancing the level and function of G0s2 could be beneficial for hypoxia- and mitochondria-related disorders, such as ischemic diseases, metabolic diseases, and cancer.

Materials and Methods

Cells were infected with adenovirus encoding FRET-based ATP indicators AT1.03 or mit-AT1.03 to measure changes in cytosolic or mitochondrial ATP concentrations, respectively. Image acquisitions and FRET analyses were performed as described previously with some modifications (13). For the control of oxygen concentration during time-lapse imaging, digital gas mixer for stage-top incubator GM8000 (Tokai Hit) was used to create hypoxic (1% O_2) or normoxic (20% O_2) condition. Additional methods are found in *SI Materials and Methods*.

ACKNOWLEDGMENTS. We thank M. Murata for helpful discussions and advice, H. Miyagi (Olympus Co. Ltd.) for technical advice regarding microscopy, T. Miyazaki (Cyclex Co. Ltd.) for making antibodies, S. Ikezawa and A. Ogai for technical assistance, K. Tanaka for help with the purification of bovine F_oF_1-ATP synthase, and Y. Okada and H. Fujii for secretarial support. This research was supported by the Japan Society for the Promotion of Science through the Funding Program for Next Generation World-Leading Researchers (NEXT Program) initiated by the Council for Science and Technology Policy; grants-in-aid from the Ministry of Health, Labor, and Welfare–Japan; and grants-in-aid from the Ministry of Education, Culture, Sports, Science, and Technology–Japan. This research was also supported by grants from Takeda Science Foundation, Japan Heart Foundation, Japan Cardiovascular Research Foundation, Japan Intractable Diseases Research Foundation, Japan Foundation of Applied Enzymology, Japan Medical Association, Uehara Memorial Foundation, Mochida Memorial Foundation, Banyu Foundation, Naito Foundation, Inoue Foundation for Science, Osaka Medical Research foundation for Intractable Diseases, Ichiro Kanehara Foundation, and Showa Houkoukai.

1. Kim JW, Tchernyshyov I, Semenza GL, Dang CV (2006) HIF-1-mediated expression of pyruvate dehydrogenase kinase: A metabolic switch required for cellular adaptation to hypoxia. *Cell Metab* 3(3):177–185.
2. Papandreou I, Cairns RA, Fontana L, Lim AL, Denko NC (2006) HIF-1 mediates adaptation to hypoxia by actively downregulating mitochondrial oxygen consumption. *Cell Metab* 3(3): 187–197.
3. Semenza GL (2012) Hypoxia-inducible factors in physiology and medicine. *Cell* 148(3): 399–408.
4. Semenza GL, et al. (1996) Hypoxia response elements in the aldolase A, enolase 1, and lactate dehydrogenase A gene promoters contain essential binding sites for hypoxia-inducible factor 1. *J Biol Chem* 271(51):32529–32537.
5. Chen YC, et al. (2012) Identification of a protein mediating respiratory supercomplex stability. *Cell Metab* 15(3):348–360.
6. Fukuda R, et al. (2007) HIF-1 regulates cytochrome oxidase subunits to optimize efficiency of respiration in hypoxic cells. *Cell* 129(1):111–122.
7. Strogolova V, Furness A, Robb-McGrath M, Garlich J, Stuart RA (2012) Rcf1 and Rcf2, members of the hypoxia-induced gene 1 protein family, are critical components of the mitochondrial cytochrome bc1-cytochrome c oxidase supercomplex. *Mol Cell Biol* 32(8):1363–1373.
8. Saks V, et al. (2006) Cardiac system bioenergetics: Metabolic basis of the Frank-Starling law. *J Physiol* 571(Pt 2):253–273.
9. Smolenski RT, Lachno DR, Ledingham SJ, Yacoub MH (1990) Determination of sixteen nucleotides, nucleosides and bases using high-performance liquid chromatography and its application to the study of purine metabolism in hearts for transplantation. *J Chromatogr A* 527(2):414–420.
10. Shimura D, et al. (2013) Metabolomic profiling analysis reveals chamber-dependent metabolite patterns in the mouse heart. *Am J Physiol Heart Circ Physiol* 305(4):H494–H505.
11. Kemp GJ, Meyerspeer M, Moser E (2007) Absolute quantification of phosphorus metabolite concentrations in human muscle in vivo by 31P MRS: A quantitative review. *NMR Biomed* 20(6):555–565.
12. Ford SR, et al. (1996) Use of firefly luciferase for ATP measurement: Other nucleotides enhance turnover. *J Biolumin Chemilumin* 11(3):149–167.
13. Imamura H, et al. (2009) Visualization of ATP levels inside single living cells with fluorescence resonance energy transfer-based genetically encoded indicators. *Proc Natl Acad Sci USA* 106(37):15651–15656.
14. Lopaschuk GD, Kelly DP (2008) Signalling in cardiac metabolism. *Cardiovasc Res* 79(2): 205–207.
15. Hattori F, et al. (2010) Nongenetic method for purifying stem cell-derived cardiomyocytes. *Nat Methods* 7(1):61–66.
16. Forsythe JA, et al. (1996) Activation of vascular endothelial growth factor gene transcription by hypoxia-inducible factor 1. *Mol Cell Biol* 16(9):4604–4613.
17. Wolf A, et al. (2011) Hexokinase 2 is a key mediator of aerobic glycolysis and promotes tumor growth in human glioblastoma multiforme. *J Exp Med* 208(2):313–326.
18. Russell L, Forsdyke DR (1991) A human putative lymphocyte G0/G1 switch gene containing a CpG-rich island encodes a small basic protein with the potential to be phosphorylated. *DNA Cell Biol* 10(8):581–591.
19. Zandbergen F, et al. (2005) The G0/G1 switch gene 2 is a novel PPAR target gene. *Biochem J* 392(Pt 2):313–324.
20. Heckmann BL, Zhang X, Xie X, Liu J (2013) The G0/G1 switch gene 2 (G0S2): Regulating metabolism and beyond. *Biochim Biophys Acta* 1831(2):276–281.
21. Dimroth P, von Ballmoos C, Meier T (2006) Catalytic and mechanical cycles in F-ATP synthases. Fourth in the Cycles Review Series. *EMBO Rep* 7(3):276–282.
22. Senior AE (2007) ATP synthase: Motoring to the finish line. *Cell* 130(2):220–221.
23. Walker JE (1998) ATP synthesis by rotary catalysis (Nobel Lecture). *Angew Chem Int Ed* 37:5000–5011.
24. Yoshida M, Muneyuki E, Hisabori T (2001) ATP synthase—a marvellous rotary engine of the cell. *Nat Rev Mol Cell Biol* 2(9):669–677.
25. Fujikawa M, Yoshida M (2010) A sensitive, simple assay of mitochondrial ATP synthesis of cultured mammalian cells suitable for high-throughput analysis. *Biochem Biophys Res Commun* 401(4):538–543.
26. Adachi K, et al. (2007) Coupling of rotation and catalysis in F(1)-ATPase revealed by single-molecule imaging and manipulation. *Cell* 130(2):309–321.
27. Itoh H, et al. (2004) Mechanically driven ATP synthesis by F1-ATPase. *Nature* 427(6973):465–468.
28. Noji H, Yasuda R, Yoshida M, Kinosita K, Jr. (1997) Direct observation of the rotation of F1-ATPase. *Nature* 386(6622):299–302.
29. Rondelez Y, et al. (2005) Highly coupled ATP synthesis by F1-ATPase single molecules. *Nature* 433(7027):773–777.
30. Uchihashi T, Iino R, Ando T, Noji H (2011) High-speed atomic force microscopy reveals rotary catalysis of rotorless F_1-ATPase. *Science* 333(6043):755–758.
31. Giorgio V, et al. (2009) Cyclophilin D modulates mitochondrial F0F1-ATP synthase by interacting with the lateral stalk of the complex. *J Biol Chem* 284(49):33982–33988.
32. Siderovski DP, Blum S, Forsdyke RE, Forsdyke DR (1990) A set of human putative lymphocyte G0/G1 switch genes includes genes homologous to rodent cytokine and zinc finger protein-encoding genes. *DNA Cell Biol* 9(8):579–587.
33. Yamada T, Park CS, Burns A, Nakada D, Lacorazza HD (2012) The cytosolic protein G0S2 maintains quiescence in hematopoietic stem cells. *PLoS ONE* 7(5):e38280.
34. Welch C, et al. (2009) Identification of a protein, G0S2, that lacks Bcl-2 homology domains and interacts with and antagonizes Bcl-2. *Cancer Res* 69(17):6782–6789.
35. Kobayashi S, et al. (2008) Expression profiling of PBMC-based diagnostic gene markers isolated from vasculitis patients. *DNA Res* 15(4):253–265.
36. Yang X, et al. (2010) The G(0)/G(1) switch gene 2 regulates adipose lipolysis through association with adipose triglyceride lipase. *Cell Metab* 11(3):194–205.

OPEN ACCESS Freely available online

PLOS ONE

Sustained-Release Delivery of Prostacyclin Analogue Enhances Bone Marrow-Cell Recruitment and Yields Functional Benefits for Acute Myocardial Infarction in Mice

Yukiko Imanishi[1], Shigeru Miyagawa[1], Satsuki Fukushima[1], Kazuhiko Ishimaru[1], Nagako Sougawa[1], Atsuhiro Saito[2], Yoshiki Sakai[3], Yoshiki Sawa[1]*

1 Department of Cardiovascular Surgery, Graduate School of Medicine, Osaka University, Osaka, Japan, **2** Medical Center for Translational Research, Osaka University Hospital, Osaka, Japan, **3** Research Headquarters, ONO Pharmaceutical CO., LTD., Osaka, Japan

Abstract

Background: A prostacyclin analogue, ONO-1301, is reported to upregulate beneficial proteins, including stromal cell derived factor-1 (SDF-1). We hypothesized that the sustained-release delivery of ONO-1301 would enhance SDF-1 expression in the acute myocardial infarction (MI) heart and induce bone marrow cells (BMCs) to home to the myocardium, leading to improved cardiac function in mice.

Methods and Results: ONO-1301 significantly upregulated SDF-1 secretion by fibroblasts. BMC migration was greater to ONO-1301-stimulated than unstimulated conditioned medium. This increase was diminished by treating the BMCs with a CXCR4-neutralizing antibody or CXCR4 antagonist (AMD3100). Atelocollagen sheets containing a sustained-release form of ONO-1301 (n = 33) or ONO-1301-free vehicle (n = 48) were implanted on the left ventricular (LV) anterior wall immediately after permanent left-anterior descending artery occlusion in C57BL6/N mice (male, 8-weeks-old). The SDF-1 expression in the infarct border zone was significantly elevated for 1 month in the ONO-1301-treated group. BMC accumulation in the infarcted hearts, detected by in vivo imaging after intravenous injection of labeled BMCs, was enhanced in the ONO-1301-treated hearts. This increase was inhibited by AMD3100. The accumulated BMCs differentiated into capillary structures. The survival rates and cardiac function were significantly improved in the ONO-1301-treated group (fractional area change 23±1%; n = 22) compared to the vehicle group (19±1%; n = 20; P = 0.004). LV anterior wall thinning, expansion of infarction, and fibrosis were lower in the ONO-1301-treated group.

Conclusions: Sustained-release delivery of ONO-1301 promoted BMC recruitment to the acute MI heart via SDF-1/CXCR4 signaling and restored cardiac performance, suggesting a novel mechanism for ONO-1301-mediated acute-MI heart repair.

Citation: Imanishi Y, Miyagawa S, Fukushima S, Ishimaru K, Sougawa N, et al. (2013) Sustained-Release Delivery of Prostacyclin Analogue Enhances Bone Marrow-Cell Recruitment and Yields Functional Benefits for Acute Myocardial Infarction in Mice. PLoS ONE 8(7): e69302. doi:10.1371/journal.pone.0069302

Editor: Toru Hosoda, Tokai University, Japan

Received February 8, 2013; **Accepted** June 6, 2013; **Published** July 19, 2013

Funding: This study was funded by grant-in-aid for Core-to-Core Program (21003) from the Japan Society for the Promotion of Science (http://jsps-osaka-u.jpn.org/en/index.html), early-stage and exploratory clinical trial centers project from the Ministry of Health (http://jsps-osaka-u.jpn.org/en/index.html), Labour and Welfare, Health and Labour Sciences Research Grant (H23-002, http://jsps-osaka-u.jpn.org/en/index.html), and from New Energy and Industrial Technology Development Organization (P10004, http://www.nedo.go.jp/english/index.html). The funders had no role in study design, data collection and analysis, decision to publish, or preparation of the manuscript.

Competing Interests: The authors have read the journal's policy and have the following conflicts: Y. Sakai was an employee of Ono Pharmaceutical Co. Ltd., and a holder of the patent for ONO-1301 encapsulated in PLGA microspheres (patent numbers WO 2004/032965 and WO 2008/047863). There are no other patents, products in development, or modified products to declare. The other authors have declared that no competing interests exist. This does not alter the authors' adherence to all PLOS ONE policies on sharing data and materials.

* E-mail: sawa@surg1.med.osaka-u.ac.jp

Introduction

Despite a number of medical and interventional treatments have been developed to treat acute myocardial infarction (AMI), the treatment for massive AMI has not been fully established. Myocardial infarction (MI) is a progressive disease, characterized by massive ischemic necrosis of the myocardial tissue and subsequent inflammation. This leads to cardiac remodeling that exacerbates the oxygen shortage in the surviving cardiac tissue. These pathological and functional deteriorations eventually cause end-stage heart failure. To delay the progression of heart failure, it is essential to suppress inflammation and fibrosis and to improve bloodflow supply in the injured myocardium consecutively. Recently, stromal cell-derived factor (SDF)-1 and its corresponding receptor CXCR4 have been shown to play prominent roles in homing of bone marrow cells (BMC) which promotes neovascularization and prevention of apoptosis via paracrine mechanism [1,2,3,4].

ONO-1301 (({5-[2-({[(1E)-phenyl(pyridin-3-yl)methylene]amino}oxy)ethyl]-7,8-dihydronaphthalen-1-yl}oxy)acetic acid) is a synthetic prostacyclin agonist. As it lacks the typical prostanoid

structure of a five-membered ring and an allylic alchol, ONO-1301 is chemically and biologically stable *in vivo*. In addition, thromboxane A2 synthethase is inhibited by ONO-1301, resulting in the promotion of endogenous prostacyclin synthesis. ONO-1301 has been reported to induce the production of endogenous hepatocyte growth factor (HGF) and vascular-endothelial growth factor (VEGF) in fibroblasts by stimulating cAMP production [5,6,7,8]. The administration of a slow-release form of ONO-1301 shows therapeutic potential, mainly due to the restoration of bloodflow in MI models of rat and swine and in a cardiomyopathic hamster [6,7,8]. The potential mechanism of the functional benefits of ONO-1301 mainly result from the enhanced secretion of growth factors, such as HGF and VEGF, which induce angiogenesis, restore bloodflow, and attenuate the progression of fibrosis. Recently we identified that ONO-1301 also upregulates SDF-1 secretion in the fibroblasts. Enhanced BMC homing in the MI heart by ONO-1301 therapy is attractive therapeutic modality. We thus hypothesized that ONO-1301 can induce BMC accumulation mediated by the upregulation of SDF-1 to elicit functional improvement in a mouse model of MI.

Methods

This study was carried out in strict accordance with the recommendations in the Guide for the Care and Use of Laboratory Animals of the National Institutes of Health. The protocol was approved by the Committee on the Ethics of Animal Experiments of the Osaka University (H23–123). All surgery was performed under sodium pentobarbital or isoflurane anesthesia, and all efforts were made to minimize suffering.

ONO-1301 and a slow-release form of ONO-1301 were purchased from ONO Pharmaceutical Co. Ltd. (Osaka, Japan) [7,8,9].

Migration Assay

Normal human dermal fibroblasts (NHDFs; Takara bio, Shiga, Japan) were cultured with or without ONO-1301 for 72 hours. The SDF-1 concentration in the culture supernatants was measured by ELISA (R&D systems, MN). BMCs were obtained from a green fluorescent protein (GFP)-transgenic mouse [C57BL/6-Tg(CAG-EGFP); Japan SLC, Inc., Shizuoka, Japan], and their migration toward the supernatants was assessed using a culture insert system (BD Falcon). The number of migrated BMCs was determined using fluorescence microscopy (Carl Zeiss, Göttingen, Germany).

Mouse AMI Model and Sheet Transplantation

An AMI model was generated by permanent ligation of the left anterior descending artery (LAD) in 10-15-week-old male C57BL/6N, BALB/cA, or BM-GFP chimera mice [10]. ONO-1301 microspheres and control microspheres were resuspended in saline at 10 mg/ml and added to atelocollagen sheets just before transplantation. Five minutes after the LAD ligation, atelocollagen sheets that included ONO-1301-containing microspheres (ONO-1301-treated group, n = 40) or empty microspheres (vehicle group, n = 40) were fixed onto the surface of the anterior left ventricular (LV) wall. The mice were euthanized 7, 21, and 28 days after the LAD ligation and ONO-1301 administration.

Assessment of BMC Homing

BMCs harvested from BALB/cA mice were labeled by Xenolight DiR (Caliper Life Sciences, MA) following the manufacturer's instructions and injected into the tail vein of BALB/cA mice after the MI and ONO-1301 treatment. On days 1 and 3, the whole-body imaging of the mice was measured by an *in vivo* imaging system (IVIS, Caliper Life Sciences).

Assessment of Cardiac Function and Survival

Cardiac function was assessed using an echocardiography system equipped with a 12-MHz transducer (GE Healthcare, WI) 4 weeks after MI and ONO-1301 treatment. The LV areas were measured, and LV fractional area change (FAC) was calculated as (LVEDA-LVESA)/LVEDA×100, where LVEDA and LVESA are the LV end-diastolic and end-systolic area, respectively.[10] The mice were housed in a temperature-controlled incubator for 28 days post-treatment to determine their survival.

Histological Analysis

Frozen sections (8 μm) of hearts were stained with antibodies against von Willebrand factor (vWF; Dako, Glostrup, Denmark) and CD31 (Abcam, UK). The secondary antibody was Alexa 546 goat anti-rabbit (Life Technologies, CA). Counterstaining was performed with 6-diamidino-2-phenylindole (DAPI; Life Technologies). The sections were also stained with isolectin (Life Technologies) following the manufacturer's instructions. To count GFP-positive cells, isolectin-positive cells, and CD31-positive capillary densities, 10 images were captured for each specimen. Capture and analysis were performed using Biorevo (Keyence, Japan). To analyze the myocardial collagen accumulation, heart sections were stained with Masson's trichrome. The collagen volume fraction in the peri-infarct area was calculated.

Quantitative Real-time PCR

The total RNA was isolated from the peri-infarct area using the RNeasy Mini Kit and reverse transcribed using Omniscript Reverse transcriptase (Qiagen, Hilden, Germany). Quantitative PCR was performed with a PCR System (Life Technologies). The expression of each mRNA was normalized to that of glyceraldehyde-3-phosphate dehydrogenase (GAPDH). The primers and probes are shown in Table S1 in File S1.

Statistical Analysis

Data are expressed as the mean ± SEM. The data distributions were checked for normality. Comparisons between 2 groups were made using the Student's *t*-test. For comparisons among 3 or more groups, one-way analysis of variance (ANOVA) followed by Fisher's protected least significant difference (PLSD) test were used. The survival curves were prepared using the Kaplan-Meier method and compared using the log-rank test. All *P*-values are two-sided, and values of $P<0.05$ were considered to indicate statistical significance. Statistical analyses were performed using the StatView 5.0 Program (Abacus Concepts, Berkeley, CA) and Statcel2 (The Publisher OMS Ltd., Saitama, Japan).

An expanded Methods section can be found in the online-only in File S1.

Results

ONO-1301 Enhanced BMC Migration via SDF-1/CXCR4 Signaling

The effect of ONO-1301 on the SDF-1 secretion by NHDFs was evaluated by ELISA. As shown in Fig. 1A, the SDF-1 concentration in the NHDF culture supernatants increased in an ONO-1301 concentration-dependent manner. The SDF-1 concentration in the culture supernatant of 1000 nM ONO-1301-treated cells was significantly greater than that of cells cultured in